Available online at www.sciencedirect.com

ScienceDirect

Ceramics International 40 (2014) 4945–4952

CERAMICS INTERNATIONAL

www.elsevier.com/locate/ceramint

Enhanced magnetic properties of substituted Sr-hexaferrite nanoparticles synthesized by co-precipitation method

Gholam Reza Gordani[a,*], Ali Ghasemi[b], Ali Saidi[a]

[a]Department of Materials Science and Engineering, Isfahan University of Technology, Isfahan, Iran
[b]Materials Engineering Department, Malek Ashtar University of Technology, Shahin Shahr, Iran

Received 14 August 2013; received in revised form 11 October 2013; accepted 22 October 2013
Available online 29 October 2013

Abstract

Nanoparticles of Mg–Co–Ti substituted strontium hexaferrite with nominal composition of $SrFe_{12-2x}(Mg,Co)_{x/2}Ti_xO_{19}$ ($x=0$–2.5) were synthesized by a co-precipitation method. The structural, magnetic and electromagnetic properties of samples were studied as a function of x by X-ray diffraction (XRD), Fourier transform infrared spectroscopy (FTIR), scanning electron microscopy (SEM), vibrating sample magnetometer (VSM) and vector network analysis. It was found that the particle size decreases with an increase in Mg–Co–Ti substitution. The XRD results showed that the crystallite size of nanoparticles lies in the range of 40–45 nm. The results of hysteresis loops indicated that for $x > 0.5$, M_s and H_c decrease with an increase in x. Vector network analysis measurements showed that the doped samples had much more effective reflection loss values than those of undoped ferrites. As a result it was found that Mg–Co–Ti doped Sr-hexaferrite can be proposed as suitable absorbers for applications in microwave technology with a good deal of consistently.

Keywords: C. Magnetic property; Nanoparticle; Strontium hexaferrite; Co-precipitation

1. Introduction

In recent years, reduction of electromagnetic backscattering and electromagnetic interference by employing microwave absorbing materials has important implications in the field of electromagnetic compatibility [1], along with the development of higher gigahertz electronics and the trend towards miniature circuitry [2,3]. In this regard, hexaferrite magnetic materials due to their large tunable anisotropy field are extensively exploited in higher gigahertz range of microwave [4,5]. Among these magnetic materials, the strontium hexaferrite nanoparticles are promising materials in this field. These materials have interesting mechanical, chemical and physical properties, especially, the magnetic properties that make it suitable for wide variety of applications such as electrical and magnetic motors, recording media and microwave absorption [6–8]. Each of these applications required special magnetic properties; hence the magnetic properties of hexaferrites must be varied to make them suitable for different industrial applications. The magnetic properties of Sr-hexaferrites such as saturation of magnetization depend on the synthesis method, particle size and the cations distribution in the magnetoplumbite crystal structure. To date, several research works have been carried out to improve the magnetic properties of Sr-hexaferrite, by substitution of magnetic and non-magnetic ions such as Co^{2+}, Mn^{2+}, Sn^{4+}, Zr^{4+} and Mg^{2+} in the Fe^{3+} site in hexaferrite structure [9–13]. Several techniques have been also employed to synthesis of Sr-hexaferrite, such as the solid state reaction route, hydrothermal [14], sol–gel [10,15], microwave induced combustion [16] and chemical co-precipitation [8]. The growing interest during the past researches is essentially the synthesis of high purity and ultrafine size of Sr-hexaferrite that having an excellent magnetic properties. Co-precipitation method is an excellent route for the preparation of purity hexaferrites due to the better homogeneity, achievable compositional control and lower synthesis temperature [17].

*Corresponding author: Tel./fax: +98 312 5912588.
E-mail address: gordani@gmail.com (G.R. Gordani).

0272-8842/$ - see front matter © 2013 Elsevier Ltd and Techna Group S.r.l. All rights reserved.
http://dx.doi.org/10.1016/j.ceramint.2013.10.096

The key work of this paper lies in the investigation of the effect of the simultaneous substitution of divalent and tetravalent cations of Mg^{2+}, Co^{2+} and Ti^{4+} on the structural, magnetic and microwave absorbing properties of Sr-hexaferrite ($SrFe_{12-2x}(Mg,Co)_{x/2}Ti_xO_{19}$) prepared by a co-precipitation method. Furthermore, the correlation between structural, magnetic and electromagnetic properties was evaluated. The measurements confirmed that the reflection loss capability of strontium hexaferrite is remarkably enhanced with an addition of Mg–Co–Ti substitutions.

2. Experimental procedure

$SrFe_{12-2x}$ $(Mg,Co)_{x/2}Ti_xO_{19}$ nanoparticles with different x (x=0.0, 0.5, 1, 1.5, 2 and 2.5) were prepared by a co-precipitation method. The stoichiometric amount of chloride compounds of Sr, Fe, Mg, Co and Ti with chemical compositions of $SrCl_2\cdot 6H_2O$, $FeCl_3\cdot 6H_2O$, $MgCl_2\cdot 6H_2O$, $CoCl_2\cdot 6H_2O$ and $TiCl_4$ were dissolved in deionized water at 70 °C to form a homogeneous solution. Then the pH of the solution was adjusted slowly to 13 by adding drop wise alkaline sodium hydroxide (NaOH 1 M) solution to form a brownish yellow suspension of the hybrid complex. The resulted gel was washed with deionized water for several time and then filtered and dried at 100 °C and then calcined at 900 °C for 1 h. The formation of substituted Sr-hexaferrite was confirmed by Fourier transform infrared spectroscopy (Tensor 27 FTIR spectrometer). The crystalline phases present in the different samples were identified by X-ray diffraction on a Philips diffractometer using Cu-$K\alpha$ radiation. The nanoparticles morphologies were observed by a VEGA/TESCAN scanning electron microscopy (SEM). The vibrating sample magnetometer (Kavir Magnet) was employed to investigate of the magnetic properties of the samples at room temperature.

Vector Network Analyzer (R&S-ZVK) was used to measure the S_{11} parameter. Therefore, the rectangular waveguide has employed and the metal plate was copper with thickness of 2 cm. Variation of the reflection loss in (dB) versus frequency was measured using an R&S vector network analyzer from 4 to 8 GHz.

The composite specimens for measurement of the reflection loss properties were prepared by mixing ferrite powders and epoxy resin with weight percentage of 70:30 and then pressed to form of cylindrical with a thickness of 1.8 mm and the diameter of 40 mm.

3. Results and discussion

3.1. Structural characteristics

The XRD patterns of the Mg, Co, and Ti doped M-type strontium hexaferrite nanoparticles in various amount of dopants are shown in Fig. 1. The main peaks of M-type strontium hexaferrite ($SrFe_{12}O_{19}$) were appeared at 2θ=30.5°, 32.4°, 34.2°, 35.8°, 37.2°, 40.5° and 42.6° revealing typical hexagonal plans of (110), (107), (114), (108), (203), (205) and (206), respectively (ICSD 00-024-1207). Well suitable crystallinity of hexaferrite

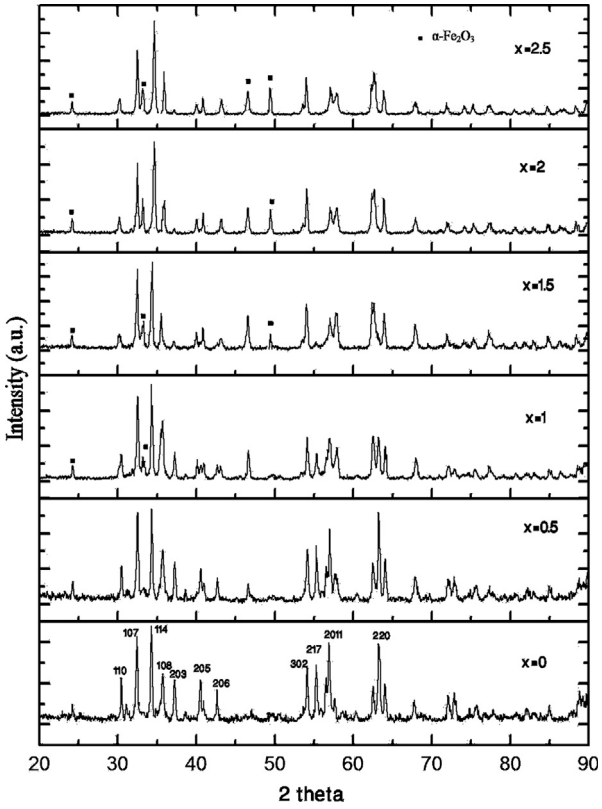

Fig. 1. XRD patterns of $SrFe_{12-2x}(Mg,Co)_{x/2}Ti_xO_{19}$ nanoparticles sintered at 900 °C for 1 h.

nanoparticles in all amount of dopants can be confirmed from sharpen peaks. In some samples, the peaks that was observed at 2θ=24.2°, 33.48°, 49.65° and 63.32° can be referred to a nonmagnetic α-Fe_2O_3 impurity phase (ICSD 00-033-0664) formed during synthesis process. It can be noted that the present impurity of α-Fe_2O_3 in final calcined samples, is due to the conversion of ferric chloride to iron hydroxide ($Fe(OH)_3$) and NaCl, followed by dehydration to form α-Fe_2O_3 as the following chemical reactions:

$$12FeCl_3+36NaOH=12Fe(OH)_3+36NaCl \quad (1)$$

$$12Fe(OH)_3=6Fe_2O_3+18H_2O \quad (2)$$

The chemical reaction between α-Fe_2O_3 and SrO obtained from dehydration of $Sr(OH)_2$, occurs at calcination temperature (900 °C) and the magnetic nanoparticles of Sr-hexaferrite are formed by the following reaction:

$$SrO+6Fe_2O_3=SrFe_{12}O_{19} \quad (3)$$

As can be seen from Fig.1, with an increase in the amount of Mg, Co and Ti contents, an additional nonmagnetic α-Fe_2O_3 phase is also appeared along with hexagonal phase. It can be noted that with substitution of Fe^{3+} ions by the Mg, Co and Ti cations in magnetoplumbite structure of $SrFe_{12}O_{19}$, some of ferric ions leave the structure and reacted with anions to form of α-Fe_2O_3 phases at high temperature [12,13].

Table 1
Structural parameters of $SrFe_{12-2x}(Mg,Co)_{x/2}Ti_xO_{19}$.

$(MgCo)_{x/2}Ti_x$ content, x	a (Å)	c (Å)	Cell volume (Å^3)	Crystallite size (nm)
0	5.872	23.01	687.55	40
0.5	5.872	23.04	688.45	43
1	5.871	23.06	688.81	40
1.5	5.870	23.10	689.77	42
2	5.872	23.12	690.84	42
2.5	5.871	23.21	693.29	45

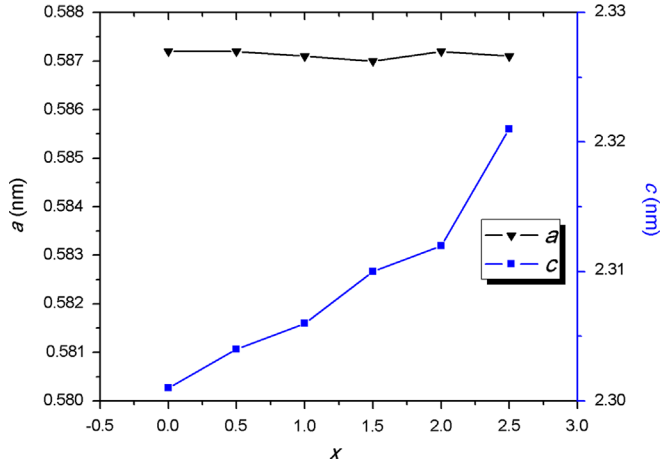

Fig. 2. Variation of lattice parameters as a function of x.

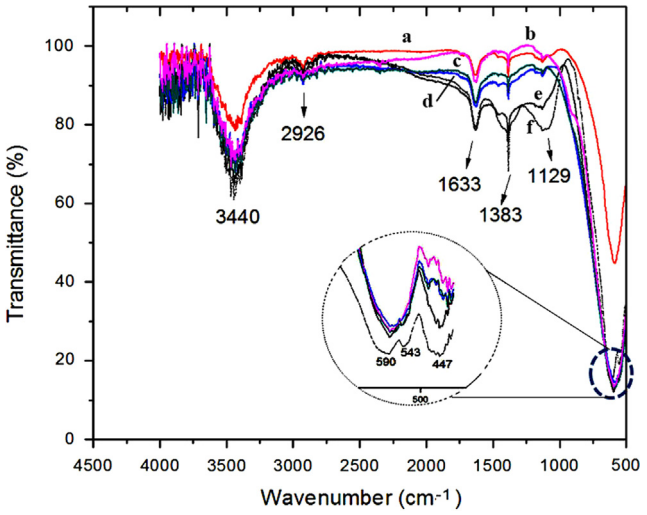

Fig. 3. FTIR spectra of the $SrFe_{12-2x}(Mg,Co)_{x/2}Ti_xO_{19}$ synthesized at 900 °C for 1 h: (a) $x=0$, (b) $x=0.5$, (c) $x=1$, (d) $x=1.5$, (e) $x=2$ and (f) $x=2.5$.

The structural parameters such as lattice constants (a and c), cell volume (v) and crystallite size are also calculated from the following equations and their values are listed in Table 1.

$$1/d^2=(4/3)((h^2+hk+k^2)/a^2)+l^2/c^2 \quad (4)$$

$$v=0.8666a^2c \quad (5)$$

The variation of lattice parameters with increasing x is shown in Fig. 2. As can be seen the lattice parameter "a" remains almost constant while the parameter "c" increases slightly from 23.01 Å to 23.21 Å and the cell volume also increases from 687.55 Å^3 to 693.29 Å^3, with an increase in the concentration of dopants in hexagonal structure.

An obvious increase in the lattice constant (c) and cell volume (v) can be related to the larger ionic radius of Mg^{2+} (0.072 nm) and Co^{2+} (0.0745 nm) compared to the ionic radius of Fe^{3+} (0.0645 nm). It must be noted that even though the ionic radius of Ti^{4+} (0.605 nm) is smaller than the other cations (Mg^{2+}, Co^{2+} and Fe^{3+}) in the samples, however it has no main influence on the variation of lattice parameters because of low amount of substitution in the structure.

Fig. 3 shows the FTIR spectrograms of the $SrFe_{12-2x}(Mg,Co)_{x/2}Ti_xO_{19}$ prepared with a co-precipitation method. It is revealed that all of samples shown have almost the same IR absorption behavior. There are obvious absorption peaks related to the asymmetric stretching and out of plane bending vibrations of the octahedral and tetrahedral sites of Sr-hexaferrites doped with Mg, Co and Ti at 436, 465, 543 and 590 cm^{-1}. The peak at 2926 cm^{-1} is ascribed to asymmetric stretching band of $-CH_2-$ that implies the existence of a C–H saturated compound with sp^3 hybridization. The relatively broad peaks at about 1630 and 3440 cm^{-1} exhibited the stretching vibration and deformation vibration of hydroxyl group (–OH) acquired from wet atmosphere. The present peaks in the range of 1100–1500 cm^{-1} referred to M–O–M bands (Metal–Oxygen–Metal) such as Co–O–Co or Fe–O–Fe bands. Additionally it can be noted that with doping of the Mg^{2+}, Co^{2+} and Ti^{4+} ions into Sr-hexaferrite the oxygen atom of Fe (Sr)–O bond might be shared with Mg, Co and Ti atoms.

Fig. 4 shows the SEM micrographs of Sr-hexaferrites samples doped with different amount of Mg, Co and Ti cations, and sintered at 900 °C for 1 h. As can be seen from Fig.4 in all the samples, the distribution of particle size is almost homogeneous and the average particle size is below 100 nm. It means that, the nucleation of particles is homogeneous and growth of them is hindered, but the nanoparticles were agglomerated. The particle size is decreased with increasing dopants concentration (i.e. increase of x). The undoped sample ($x=0$) has largest particle size (94 nm) and the configuration is almost platelet shape. The sample with $x=2.5$ has the smallest particle size of 45 nm and the configuration is almost spherical shape. In other words, with an increase in the amount of dopants typical particle morphologies are gradually varied from platelet shape to spherical.

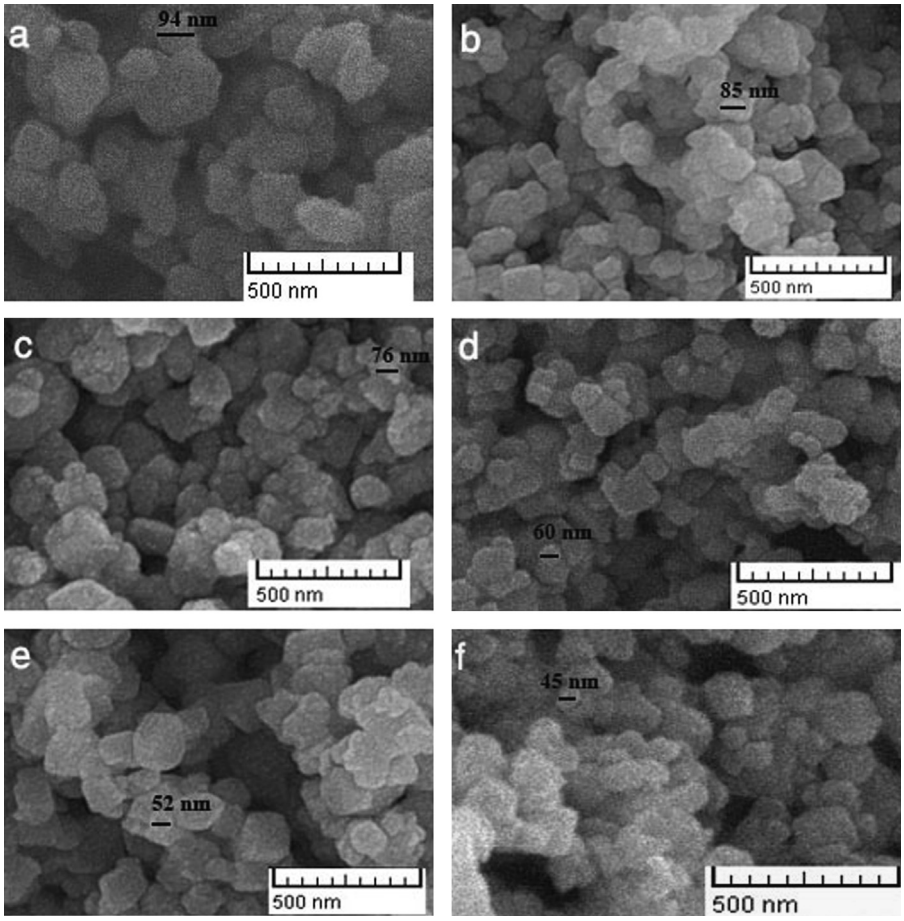

Fig. 4. SEM micrographs of $SrFe_{12-2x}(Mg,Co)_{x/2}Ti_xO_{19}$: (a) $x=0$, (b) $x=0.5$, (c) $x=1$, (d) $x=1.5$, (e) $x=2$, and (f) $x=2.5$, sintered at 900 °C for 1 h.

The similar trend for morphological evolution was also observed in Mn–Co–Sn substituted Ba-hexaferrite [18].

It is reported that the pH of precursors influences on the morphologies of nanoparticles in co-precipitation synthesizing method [19]. With an increase in concentration of dopants, the pH of solvent is decreased and subsequently, high amount of the agent (e.g. NaOH) is required to reach the suitable pH of precipitation. Therefore the nucleation rate of precipitation and subsequently the nanoparticles morphologies are varied from one sample to another.

3.2. Magnetic properties of doped Sr-hexaferrite nanoparticles

The magnetic hysteresis loops of M-type strontium hexaferrite doped with different amount of Mg, Co and Ti are shown in Fig. 5.

Fig. 5 depicts that with an increase in amount of x, the saturation of magnetization (M_s) decreases from 39.55 to 19.27 emu/g, except in $x=0.5$ (40 emu/g), while the magnetic remanence (M_r) decreases in all the samples. The decreasing of M_s and M_r cannot be only related to the increasing of the non-magnetic phases in doped Sr-hexaferrite such as α-Fe_2O_3, but also can be explained on the basis of the occupation of the substituted ions. There are five substitutional sites in the magnetoplumbite structure of Sr-hexaferrite. The sites of $12k$, $2a$ and $2b$ have upward spin direction, while $4f_1$ and $4f_2$ sites have downward spin direction. Thus, the magnetic moment per formula of magnetoplumbite Sr-hexaferrite can be expressed as follows [20]

$$m=(2a)^{\rightarrow}+(2b)^{\rightarrow}+(12k)^{\rightarrow}+(4f_1)^{\leftarrow}+(4f_2)^{\leftarrow} \quad (6)$$

The Ti^{4+} and Mg^{2+} are nonmagnetic while Co^{2+} has the magnetic moment of 3 μB which is smaller than that of the Fe^{3+} (5 μB). According to previous literature [21] the magnetic moment per Fe^{3+} ion is various in each substitutional site, that can be calculated from Mossbauer spectroscopy. Subsequently, the magnetic moments of Co^{2+} ions can be expressed by the following equation:

$$\mu_i=\mu_i(Fe^{3+})+\mu_i(Co^{2+}) \quad (7)$$

where $\mu_i(Fe^{3+})$ and $\mu_i(Co^{2+})$ are the magnetic moments of Fe^{3+} and Co^{2+} ions, respectively, in the ith sublattice. The increase of saturation of magnetization in $x \leq 0.5$, may be due to the replacement of $4f_1$ and $4f_2$ spin-down Fe^{3+} ions by non-magnetic (Mg^{2+}, Ti^{4+}) and magnetic ions (Co^{2+}), respectively, based on Eq. (6), however, further investigations are needed in this field.

In the higher content of x ($x > 0.5$), the spin-up Fe^{3+} ions in the $2a$, $2b$ and $12k$ sites can be replaced by non-magnetic

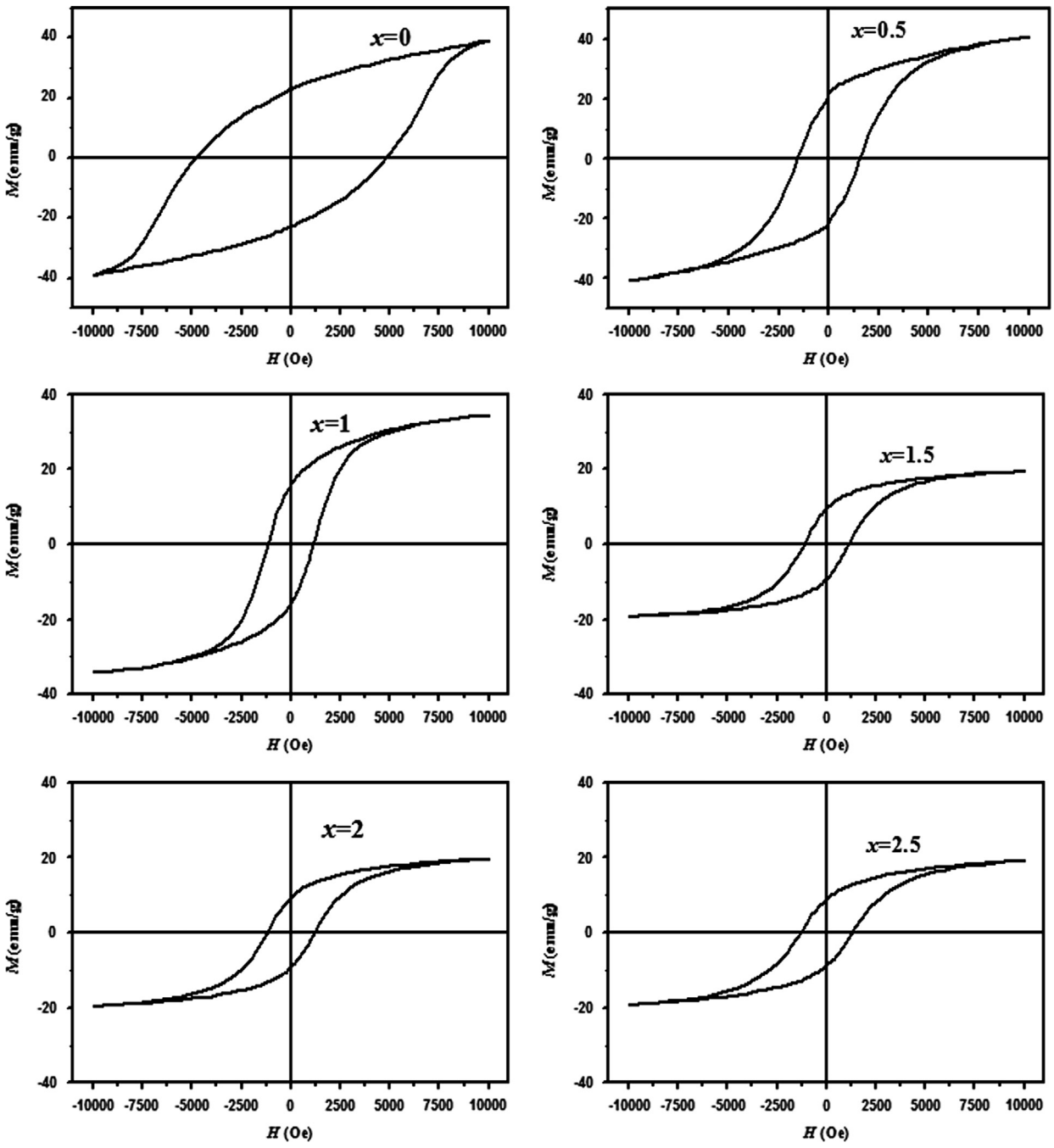

Fig. 5. Magnetic hysteresis loops of $SrFe_{12-2x}(Mg,Co)_{x/2}Ti_xO_{19}$ with various composition.

Mg^{2+} and Ti^{4+} ions and Co^{2+} (because of its lower magnetic moment rather than Fe^{3+}), especially the 12*k* octahedral site. The cations of Mg, Co and Ti as dopants have a strong influence on coercive force of M-type Sr-hexaferrite.

Fig. 6 shows the variation behavior of coercivity (H_c) of the doped Sr-hexaferrite with an increase in amount of x.

As can be seen from Fig. 6, the coercivity of $SrFe_{12-2x}(Mg,Co)_{x/2}Ti_xO_{19}$ ($x=0$–2.5) is abruptly decreased from 4.8 kOe for $x=0$ to 1.58 kOe for $x=0.5$ and then continuously decreased to 1.1 kOe for $x=2$. The coercivity (H_c) is linearly related to the reciprocal of particle size [22] and also is dependent of magnetocrystalline anisotropy as the following equation:

$$H_a = H_c = 2K_1/M_s \tag{8}$$

where K_1 is the anisotropy constant and M_s is the saturation of magnetization. Consequently, it is concluded that with decreasing of particle size, the coercivity is increased. On the contrary of expectation, it was found from SEM micrographs and VSM results, that the coercivity has straightforward relation with particle size, consequently another main parameter namely anisotropy constant has the main impact on the variation of

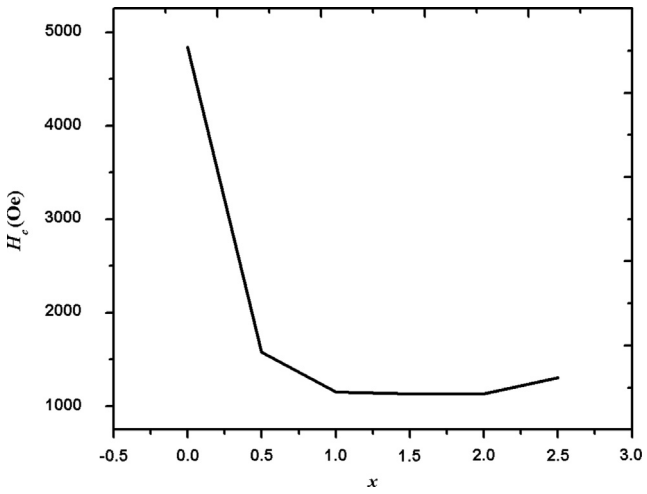

Fig. 6. Influence of the amount of x on the H_c of the $SrFe_{12-2x}(Mg,Co)_{x/2}Ti_xO_{19}$ nanoparticles.

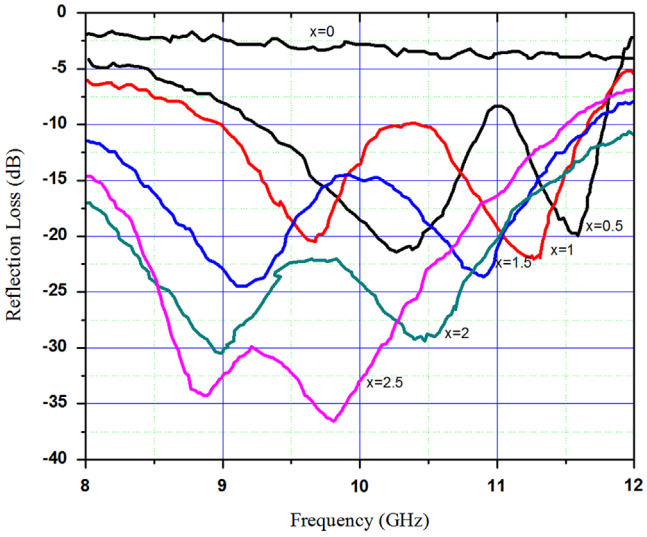

Fig. 7. Reflection loss versus frequency in the $SrFe_{12-2x}(Mg,Co)_{x/2}Ti_xO_{19}$ with different amount of x.

coercivity. It has been reported that in strontium hexaferrite the $12k$, $4f_2$ and $2b$ sites are the major contributor to the magnetocrystalline anisotropy [23]. As mentioned above, the Ti^{4+} has tendency to occupy the $12k$ and partially $4f_2$ sites. Also, Mg^{2+} occupies the $2b$ and $12k$ sites and Co^{2+} has preferred to occupy the $4f_2$ and $2a$ sites for Fe^{3+} in M-type phase, and as a result it causes negative impact on the magnetocrystalline anisotropy consequently the coercivity decreased, however, further studies are needed to confirm this.

3.3. Microwave absorption properties

The variation of the measured reflection losses (RL) of the substituted Sr-hexaferrite samples with various amount of Mg–Co and Ti cations ($x=0$, 0.5, 1, 1.5, 2, and 2.5) in the frequency range of 8–12 GHz is shown in Fig.7. Table 2 lists the data of reflection loss properties for the absorbing composites. As can be seen from Fig. 7 the whole series of samples contain two resonance peaks except undoped Sr-hexaferrite sample ($x=0$). The maximum attenuation of the incident electromagnetic wave occurs at resonance peaks. It is known that the ferrimagnetic resonance frequency of strontium hexaferrite (~48 GHz) is much larger than X-band frequencies (8–12 GHz) due to its large magnetocrystalline anisotropy [24]. Consequently the undoped sample does not have any resonance peak in X-band frequencies and its reflection loss (RL) is almost constant in the frequency range of 8–12 GHz.

As can be seen from Fig. 7, for $x>0$, with an increase of the substitution amount of cations in Sr-hexaferrite the frequencies of the minimum reflection loss are shifted to lower frequencies. The minimum of reflection loss also decreases from –21.6 dB for $x=0.5$ to −36.78 dB for $x=2.5$, indicated that the reflection loss properties of Sr-hexaferrite were enhanced with increase an amount of Mg, Co and Ti substitution cations in magnetoplumbite structure of Sr-hexaferrite.

Doping of Sr-hexaferrite with magnetic and nonmagnetic cations causes to the reducing of resonance frequency according to the ferrimagnetic resonance theory

$$f=(\gamma/2\pi)H_a \quad (9)$$

where γ is the gyromagnetic ratio and H_a is anisotropy field. With an increase in x value, the anisotropy constant (K_1) and crystalline anisotropy field (H_a) are decreased as shown in Eq. (8).

The first anisotropy constant of the sample was also measured by magneto-torque meter and listed in Table 3. It can be observed that the first anisotropy constant values are decreased with an increase in Mg–Co–Ti cations in the Sr-hexaferrite samples. Consequently the resonance frequency of doped Sr-hexaferrite samples is decreased to lower values in comparison to undoped sample. According to Chen et al. [25], a suitable microwave absorption material should have low reflection loss and wide frequency bandwidth, in which the reflection loss is higher than −10 dB. It can be seen from

Table 2
Microwave absorption properties of $SrFe_{12-2x}(Mg,Co)_{x/2}Ti_xO_{19}$.

Composition (x)	Minimum RL value (dB)	Frequency of minimum RL (GHz)	Bandwidth (GHz) (RL < −10 dB)
0	–	–	–
0.5	−21.6	10.26	2.27
1	−22.2	11.27	2.45
1.5	−24.59	9.13	3.69
2	−30.64	8.99	4
2.5	−36.78	9.8	3.5

Table 3
First anisotropy constant of $SrFe_{12-2x}(Mg,Co)x_{/2}Ti_xO_{19}$ samples with different dopant contents (x).

	$x=0$	$x=0.5$	$x=1$	$x=1.5$	$x=2$	$x=2.5$
K_1 ($\times 10^5$ erg/g)	5.36	3.65	1.98	0.53	−0.95	−1.01

Fig. 7 that by adding the substitution amount to $x=2$, the absorption bandwidth increases from 2.27 GHz for $x=0.5$–4 GHz for $x=2$. The ferrite with composition of $SrFe_8MgCoTi_2O_{19}$ exhibits the widest bandwidth than that obtained from other samples. The maximum of reflection loss of this band is -30.64 dB at matching frequency of 8.99 GHz and also there is another matching frequency at 10.47 GHz with reflection loss of -29.55 dB. This dispersion is due to the domain wall motion resonance at lower frequency and natural resonance at higher frequency, respectively. With a further increase of $x>2$, the absorption bandwidth is decreased. However, the highest reflection loss is related to the ferrite with $x=2.5$ (-36.78 dB at 9.8 GHz). Generally when the size of nanoparticles belongs to the nanoscale range, the quantum confine effect makes the microwave-absorbing properties of nanoferrite change greatly. According to the Kubo theory [26], the energy levels in nanoparticles are not continuous but split because of the quantum confine effect. When an energy level is in the range of microwave energy, the electron will absorb a photon to hop from a low energy level to a higher one. In our work, the nanoparticles is large enough (45–94 nm), so that the quantum confine effect cannot be acted as an absorption mechanism. The defects and interfaces can also cause multiple scattering and interface polarization, which result in the electromagnetic wave absorption. In other words, the repetition reflection of the incident wave between nanoparticles will cause more energy absorption of microwave.

Previous literature in the field has reported that the minimum reflection loss reaches to -43 dB, however with narrower bandwidth of 1.8 GHz [27]. The present study shows the Mg–Co–Ti substituted Sr-hexaferrite with proper substitution amount has related excellent absorption properties such as minimum of reflection loss of -36.78 dB with more than 4 GHz absorption bandwidth.

4. Conclusions

Nanoparticles of $SrFe_{12-2x}(Mg,Co)_{x/2}Ti_xO_{19}$ ferrites were synthesized successfully by a co-precipitation method. The structural and magnetic results indicated that the amount of dopants of Mg, Co and Ti cations has a strong influence on crystalline parameters, saturation of magnetization and coercivity of samples. With an increase in x value, the lattice parameter "a" was constant and the lattice parameter "c" decreased slightly from 23.01 Å to 22.80 Å. Average particle size tends to decrease from 94 nm for $x=0$ to 45 nm for $x=2.5$ and assuming more of a spherical shape appearance. With an increase in x ($0<x<2$) the coercivity abruptly falls at first ($x\leq 0.5$), and then gradually decreased ($x>0.5$). Based on microwave measurements, the doped Sr-hexaferrites have better reflection loss property than that of undoped one. The resonance frequencies were shifted from 10.26 GHz with minimum RL value of -21.6 dB (for $x=0.5$) to 9.8 GHz with minimum RL value of -36.78 dB (for $x=2.5$). The frequencies corresponding to the minimum reflection loss of $SrFe_{12-2x}(Mg,Co)_{x/2}Ti_x\ O_{19}$ shows an inverse relationship with the increase in amount of dopants. The $SrFe_8(Mg,Co)Ti_2O_{19}$ ($x=2$) nanoparticles can be used as a potential magnetic loss material for X-band, with microwave absorption greater than 90% (reflectivity ≤ -10 dB) at frequency range of 8–12 GHz.

References

[1] D.D.L. Chung, Electromagnetic interference shielding effectiveness of carbon materials, Carbon 39 (2001) 279–285.

[2] S.B. Cho, D.H. Kang, J.H. Oh, Relationship between magnetic properties and microwave-absorbing characteristics of NiZnCo ferrite composites, J. Mat. Sci. 31 (17) (1996) 4719–4722.

[3] A.N. Yusoff, M.H. Abdullah, S.H. Ahmad, S.F. Jusoh, A.A. Mansor, S. A.A. Hamid, Electromagnetic and absorption properties of some microwave absorbers, J. Appl. Phys. 92 (2002) 876–882.

[4] A. Ghasemi, A. Morisako, Structural and electromagnetic characteristics of substituted strontium hexaferrite nanoparticles, J. Magn. Magn. Mater. 320 (2008) 1167–1172.

[5] P. Singh, V.K. Babbar, A. Razdan, R.K. Puri, T.C. Goel, Complex permittivity, permeability, and X-band microwave absorption of CaCoTi ferrite composites, J. Appl. Phys. 87 (9) (2000) 4362–4366.

[6] Q. Fang, H. Cheng, K. Huang, J. Wang, R. Li, Y. Jiao, Doping effect on crystal structure and magnetic properties of chromium-substituted strontium hexaferrite nanoparticles, J. Magn. Magn. Mater. 294 (2005) 281–286.

[7] P. Veverka, K. Knizek, E. Pollert, J. Bohacek, S. Vasseurc, E. Duguetc, J. Portier, Strontium ferrite nanoparticles synthesized in presence of polyvinylalcohol: phase composition, microstructural and magnetic properties, J. Magn. Magn. Mater. 309 (2007) 106–112.

[8] M.N. Ashiq, M.J. Iqbal, I.H. Gul, Structural, magnetic and dielectric properties of Zr–Cd substituted strontium hexaferrite ($SrFe_{12}O_{19}$) nanoparticles, J. Alloys Compd. 487 (2009) 341–345.

[9] Z. Zhang, X. Liu, X. Wang, Y. Wu, R. Li, Effect of Nd–Co substitution on magnetic and microwave absorption properties of $SrFe_{12}O_{19}$ hexaferrites, J. Alloys Compd. 525 (2012) 114–119.

[10] Q. Fang, Y. Liu, P. Yin, X. Li, Magnetic properties and formation of Sr ferrite nanoparticle and Zn, Ti/Ir substituted phases, J. Magn. Magn. Mater. 234 (2001) 366–370.

[11] M.J. Iqbal, M.N. Ashiq, P. Hernández-Gómez, J.M. Muñoz, C.T. Cabrera, Influence of annealing temperature and doping rate on the magnetic properties of Zr–Mn substituted Sr-hexaferrite nanoparticles, J. Alloys Compd. 500 (2010) 113–116.

[12] A. Ghasemi, X. Liu, A. Morisako, Effect of additional elements on the structural properties, magnetic characteristics and natural resonance frequency of strontium ferrite nanoparticles/polymer composite, IEEE Trans. Magn. 45 (10) (2009) 4420–4423.

[13] P.G. Bercoff, C. Hermeb, S.E. Jacobo, The influence of Nd–Co substitution on the magnetic properties of non-stoichiometric strontium hexaferrite nanoparticles, J. Magn. Magn. Mater. 321 (2009) 2245–2250.

[14] J. Malick, N. Virginie, B. Julien, J.M. Le Breton, Synthesis and characterization of $SrFe_{12}O_{19}$ powder obtained by hydrothermal process, J. Alloys Compd. 496 (2010) 306–312.

[15] M.G. Hasab, S.A.S. Ebrahimi, A. Badiei, An investigation on physical properties of strontium hexaferrite nanopowder synthesized by a sol–gel auto-combustion process with addition of cationic surfactant, J. Eur. Ceram. Soc. 27 (2007) 3637–3640.

[16] Y.P. Fu, C.H. Lin, Fe/Sr ratio effect on magnetic properties of strontium ferrite powders synthesized by microwave induced combustion processed, J. Alloys Compd. 386 (2005) 222–227.

[17] H. Hsiang, R.Q. Yao, Hexagonal ferrite powder synthesis using chemical coprecipitation, Mater. Chem. Phys. 104 (2007) 1–4.

[18] Y. Liu, M.G.B. Drew, Y. Liu, Preparation and magnetic properties of barium ferrites substituted with manganese, cobalt and tin, J. Magn. Magn. Mater. 323 (2011) 945–953.

[19] A. Davoodi, B. Hashemi, Magnetic properties of Sn–Mg substituted strontium hexaferrite nanoparticles synthesized via coprecipitation method, J. Alloys Compd. 509 (2011) 5893–5896.

[20] I. Bsoul, S.H. Mahmood, A.F. Lehlooh, Structural and magnetic properties of $BaFe_{12-2x}Ti_xRu_xO_{19}$, J. Alloys Compd. 498 (2010) 157–161.
[21] H. Luo, B.K. Rai, S.R. Mishra, V.V. Nguyen, J.P. Liu, Physical and magnetic properties of highly aluminum doped strontium ferrite nanoparticles prepared by auto-combustion route, J. Magn. Magn. Mater. 324 (2012) 2602–2608.
[22] J. Dho, E.K. Lee, J.Y. Park, N.H. Hur, Effects of the grain boundary on the coercivity of barium ferrite $BaFe_{12}O_{19}$, J. Magn. Magn. Mater. 285 (2005) 164–168.
[23] Z. Yang, C.S. Wang, X.H. Li, H.X. Zeng, (Zn, Ni, Ti) substituted barium ferrite particles with improved temperature coefficient of coercivity, Mater. Sci. Eng. B 90 (2002) 142–145.
[24] F. Tabatabaie, M.H. Fathi, A. Saatchi, A. Ghasemi, Effect of Mn–Co and Co–Ti substituted ions on doped strontium ferrites microwave absorption, J. Alloys Compd. 474 (2009) 206–209.
[25] N. Chen, K. Yang, M.Y. Gu, Microwave absorption properties of La-substituted M-type strontium ferrites, J. Alloys Compd. 490 (2010) 609–612.
[26] A. Kawabata, R. Kubo, Electronic properties of fine metallic particles. II. Plasma resonance absorption, J. Phys. Soc. Jpn. 21 (1966) 1765–1772.
[27] A. Sharbati, S. Choopani, A. Mousavi Azar, M. Senna, Structure and electromagnetic behavior of nanocrystalline $SrMg_xZr_xFe_{12-2x}O_{19}$ in the 8–12 GHz frequency range, Sol. St. Commun. 150 (2010) 2218–2222.